Обзор ArXiv/astro-ph, 5-9 апреля 2021 года

От Сильченко О.К.

ArXiv: 2104.03099

The ALPINE-ALMA [CII] Survey: Kinematic Diversity & Rotation in Massive Star Forming Galaxies at z ~ 4.4 – 5.9

G. C. Jones[1,2]★, D. Vergani[3], M. Romano[4,5], M. Ginolfi[6], Y. Fudamoto[7], M. Béthermin[8], S. Fujimoto[9,10], B. C. Lemaux[11], L. Morselli[4,5], P. Capak[12], P. Cassata[4], A. Faisst[12], O. Le Fèvre[8], D. Schaerer[13], J. D. Silverman[14,15], Lin Yan[16], M. Boquien[17], A. Cimatti[18,19], M. Dessauges-Zavadsky[13], E. Ibar[20], R. Maiolino[1,2], F. Rizzo[9,10], M. Talia[3,18], G. Zamorani[3]

[1]*Cavendish Laboratory, University of Cambridge, 19 J. J. Thomson Ave., Cambridge CB3 0HE, UK*
[2]*Kavli Institute for Cosmology, University of Cambridge, Madingley Road, Cambridge CB3 0HA, UK*
[3]*INAF - Osservatorio di Astrofisica e Scienza dello Spazio, via Gobetti 93/3 - 40129, Bologna - Italy*
[4]*Dipartimento di Fisica e Astronomia, Universitá di Padova, vicolo dell'Osservatorio 3, I-35122 Padova, Italy*
[5]*INAF - Osservatorio Astrofisico di Padova, vicolo dell'Osservatorio 5, I-35122 Padova, Italy*
[6]*European Southern Observatory, Karl-Schwarzschild-Str. 2, D-85748, Garching, Germany*
[7]*Research Institute for Science and Engineering, Waseda University, Tokyo 169-8555, Japan*
[8]*Aix-Marseille Université, CNRS, LAM, Laboratoire d'Astrophysique de Marseille, Marseille, France*
[9]*Cosmic Dawn Center (DAWN), Jagtvej 128, DK2200, Copenhagen N, Denmark*
[10]*Niels Bohr Institute, University of Copenhagen, Lyngbyvej 2, DK2100 Copenhagen Ø, Denmark*
[11]*Department of Physics & Astronomy, University of California, Davis, One Shields Ave., Davis, CA 95616, USA*
[12]*Infrared Processing and Analysis Center, California Institute of Technology, Pasadena, CA 91125, USA*
[13]*Observatoire de Genève, Université de Genève, 51 Ch. des Maillettes, 1290 Versoix, Switzerland*
[14]*Kavli Institute for the Physics and Mathematics of the Universe, The University of Tokyo Kashiwa, Chiba 277-8583, Japan*
[15]*Department of Astronomy, School of Science, The University of Tokyo, 7-3-1 Hongo, Bunkyo, Tokyo 113-0033, Japan*
[16] *The Caltech Optical Observatories, California Institute of Technology, Pasadena, CA 91125, USA*

Обзор ALPINE: статистика выборки?

Addressing this lack of kinematically characterized galaxies at $z > 4$ was one of the main driving goals of the ALMA Large Program to INvestigate CII at Early Times (ALPINE; Le Fèvre et al. 2020; Béthermin et al. 2020; Faisst et al. 2020). This survey observed 118 galaxies at $z = 4.4 - 5.9$ in [CII] 158μm and the surrounding rest-frame FIR emission, following the success of the pilot program (Capak et al. 2015) and increasing the number of such observations by an order of magnitude. Source selection was based on UV luminosity ($L_{UV} > 0.6L^*$), pre-existing spectroscopic redshifts, and lack of type 1 AGN. ALPINE sources lie on the star forming main sequence (e.g., Noeske et al. 2007; Faisst et al. 2020) and are thus broadly representative of the underlying population of galaxies at these redshifts.

In this work, we examine the 75 [CII]-detected galaxies in the ALPINE survey using tilted ring models and morpho-kinematic classification criteria, with the goals of studying the kinematic diversity of this unique sample, testing the applicability of low-redshift classification criteria to high-redshift observations, and characterizing the properties (e.g., rotation curves, morphological parameters, velocity

Each cube was continuum-subtracted in the *uv*-plane using the CASA task UVCONTSUB, resulting in a line-only, continuum-free data cube. Since the restoring beam of each observation was comparable (average of $1.13'' \times 0.85''$, Béthermin et al. 2020), each image was created using a uniform cell size of $0.15''$. The line cubes were constructed with channels of $25\,\mathrm{km\,s^{-1}}$, or $\sim 30\,\mathrm{MHz}$. All cubes were cleaned down to 3σ (CASA TCLEAN) and were created using natural weighting.

These continuum-subtracted cubes were searched for signal using a custom line search algorithm, resulting in the detections of 75 [CII]-emitting galaxies (Béthermin et al. 2020). To examine the morpho-kinematic diversity of this sample, the [CII] channel maps, integrated intensity (moment 0) maps, velocity fields (moment 1), position-velocity diagrams (PVDs) along the major and minor axes, integrated spectra, and ancillary photometry (Faisst et al. 2020) were inspected by a team within the ALPINE collaboration (Le Fèvre et al. 2020). Based on this information, each member independently classified each galaxy as rotating (class 1), merging (class 2), extended dispersion-dominated (class 3), compact dispersion-dominated (class 4), or too weak to characterize (class 5), and the class for each galaxy was agreed upon.

The five morpho-kinematic classes of Le Fèvre et al. (2020) contain 9, 31, 15, 8, and 12 galaxies (75 total) for classes 1 through 5, respectively. Of these sources, we recover 6, 21, 13, 0, and 0 galaxies, respectively (40 total). The total lack of compact or weak (class 4 or 5, respectively) galaxies is explained by the algorithm criteria noted above. However, we do recover $\sim 67 - 87\%$ of the sources originally classified into classes 1-3.

На самом деле, у них осталось 29 галактик…

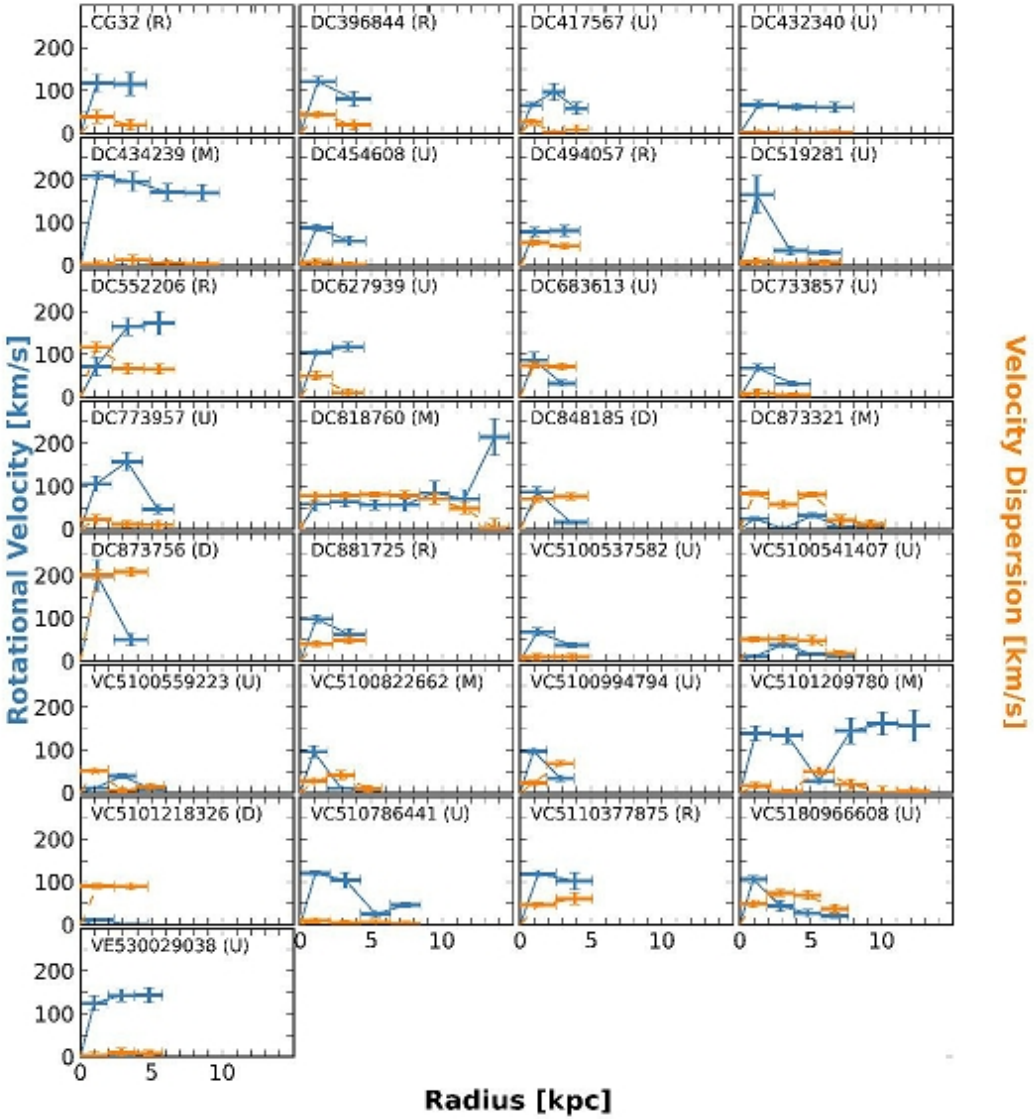

Свойства выборки

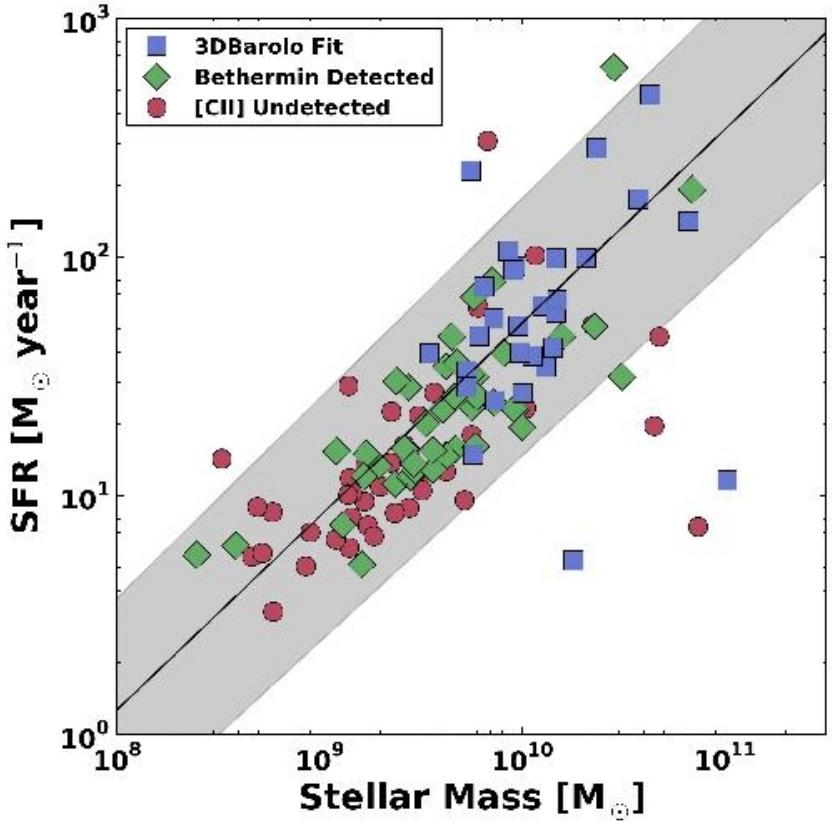

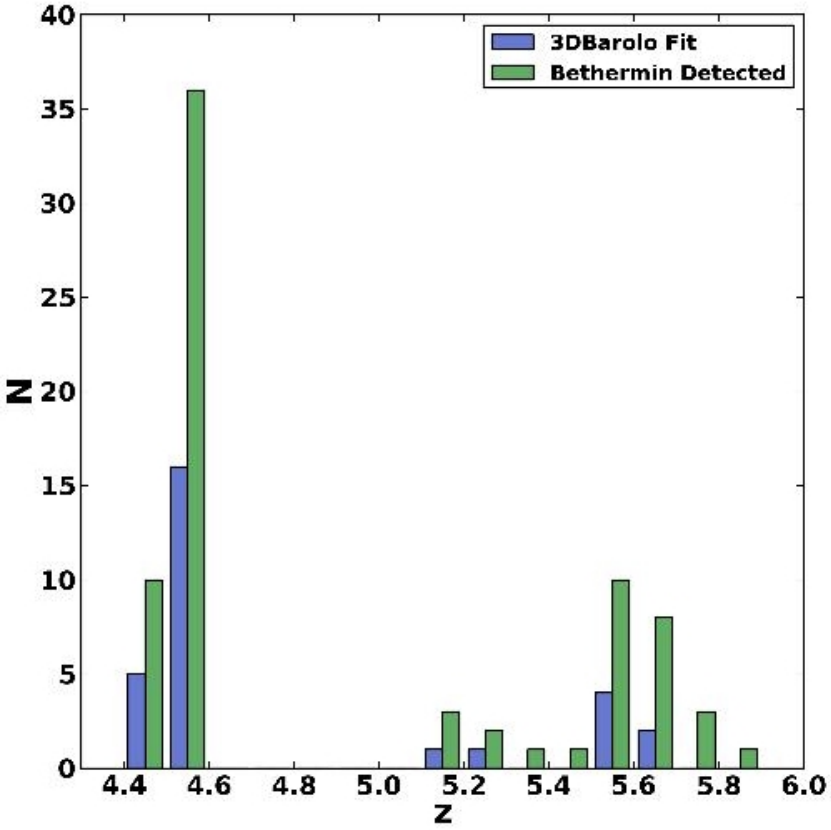

Примеры подклассов: 6:3

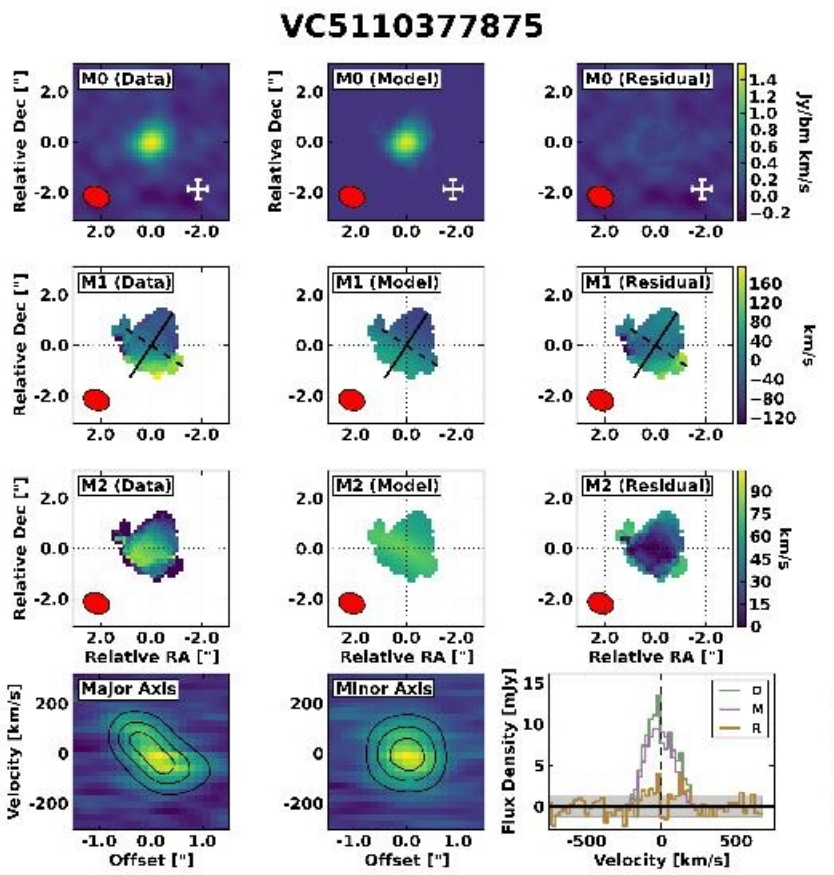

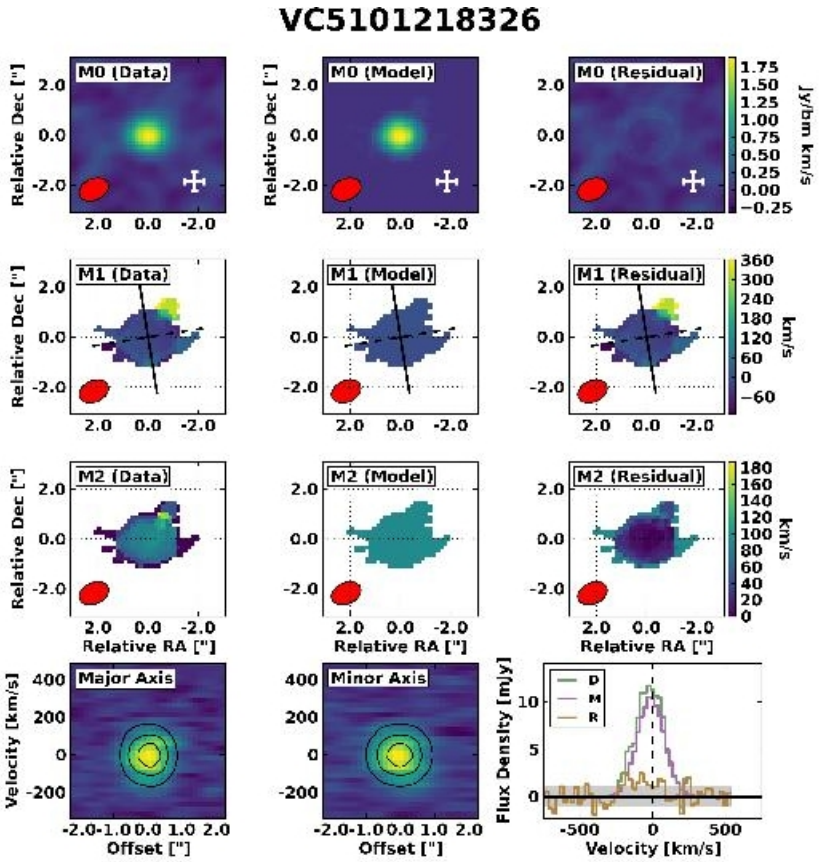

ротаторы

дисперсеры

Примеры подклассов: 5:15

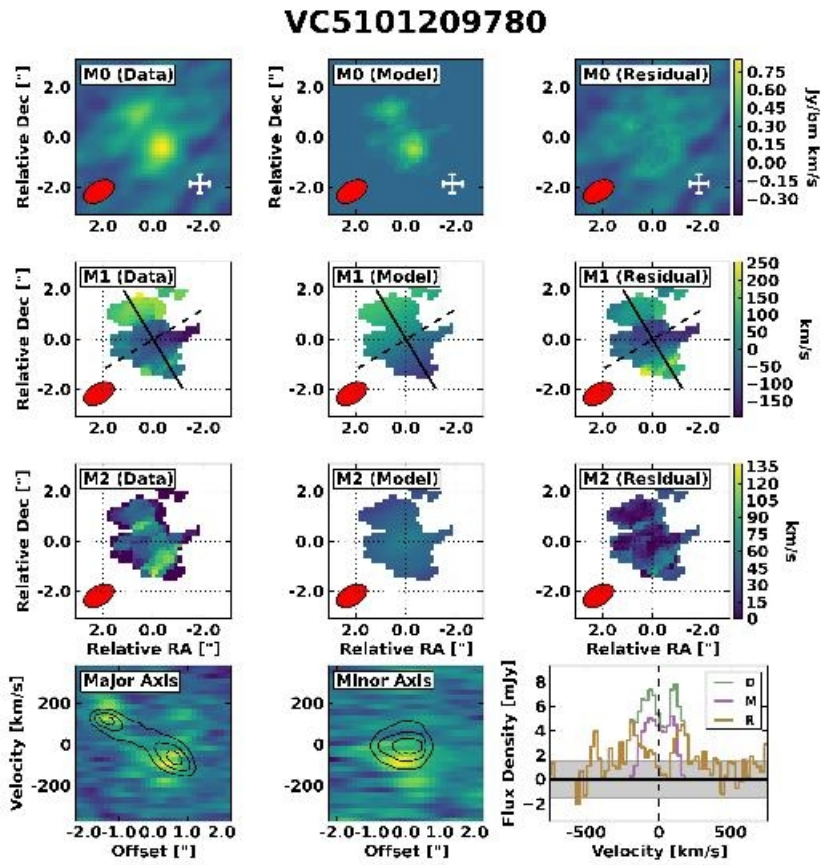

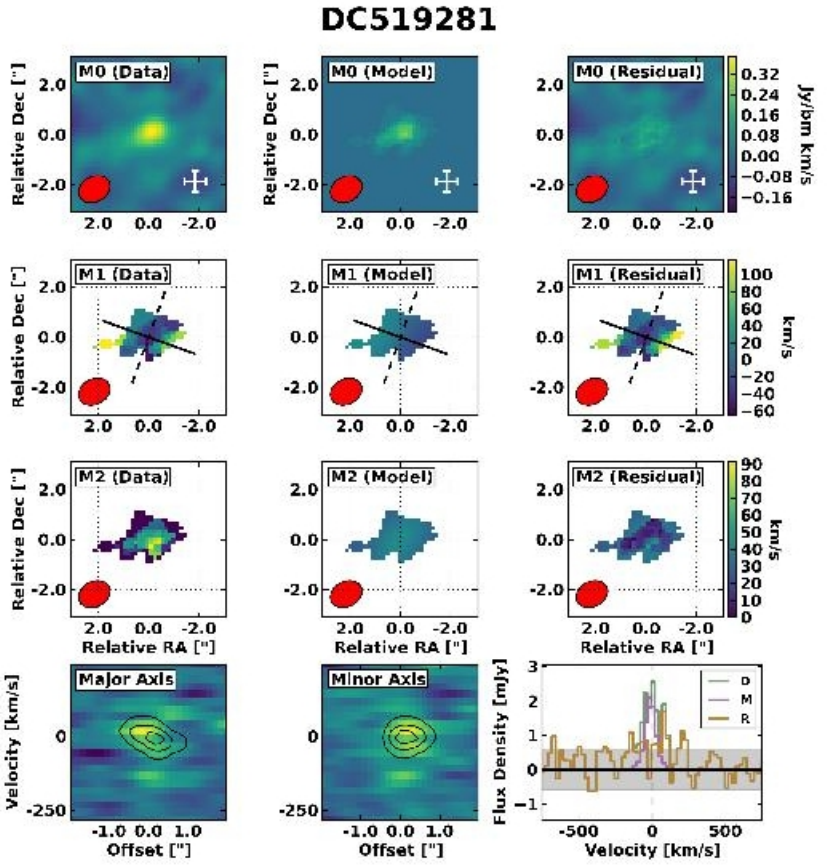

мержеры

непонятно что

По дороге лягнули чисто морфологическую классификацию

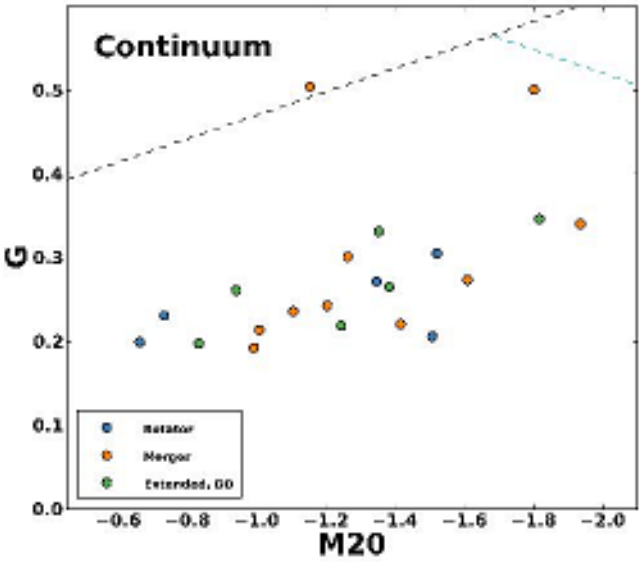

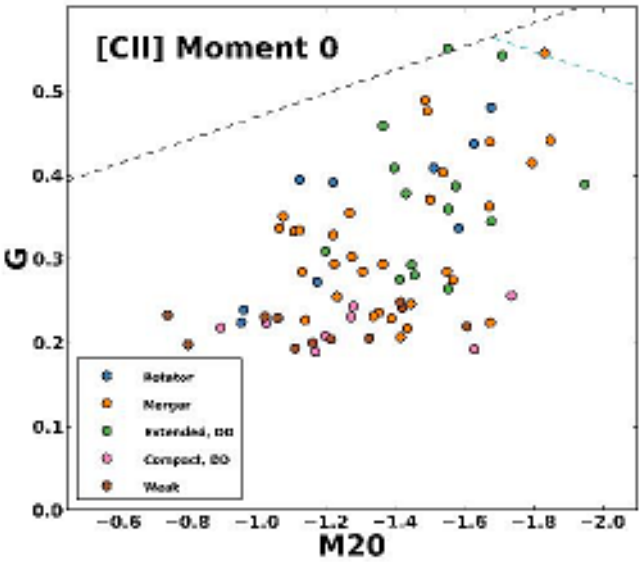

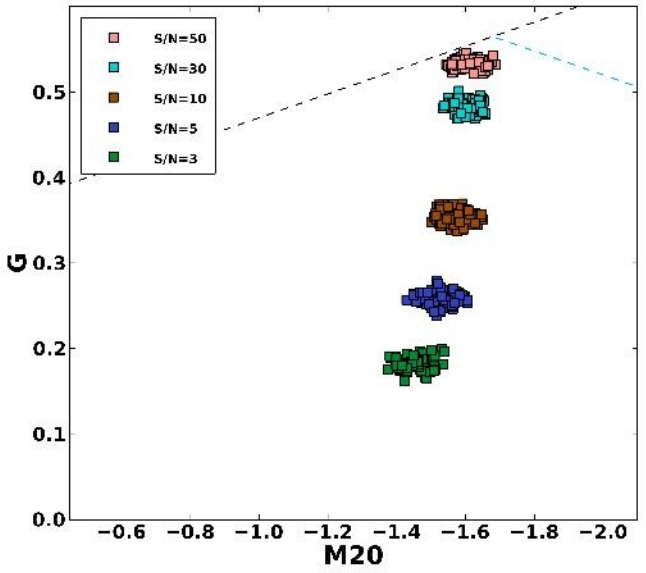

Figure 5. G-M_{20} for a set of model point sources convolved with a 2-D Gaussian beam. For each of the 118 ALPINE synthesized beams, we explore five upper SNR thresholds (3, 5, 10, 30, 50) for SNR_{lower} = 1.0. Dashed lines represent morphological regions of Lotz et al. (2008), where the upper region contains mergers, the right region contains E/S0/Sa galaxies, and the lower region contains Sb-Irr.

Результаты

Name	z	PA_M [°]	PA_K [°]	i_M [°]	i_K [°]	W15 1	2	3	4	5	KC1 L20	KC2 J21
CG32	4.41	90 ± 60	238 ± 14	50 ± 20	56 ± 19	✓	✓	✓	×	✓	2	ROT
DC396844	4.542	161 ± 28	197 ± 14	60 ± 19	57 ± 31	✓	✓	×	×	×	1	ROT
DC417567	5.67	160 ± 80	49 ± 4	40 ± 50	68 ± 13	✓	✓	✓	×	✓	2	UNC
DC432340	4.404	11 ± 18	187 ± 8	59 ± 19	67 ± 12	✓	✓	✓	✓	✓	2	UNC
DC434239	4.488	28 ± 8	218 ± 3	63 ± 8	73 ± 13	✓	✓	×	✓	×	2	MER
DC454608	4.584	140 ± 40	193 ± 9	67 ± 25	56 ± 9	×	✓	×	×	×	2	UNC
DC494057	5.545	60 ± 90	185 ± 14	31 ± 25	46 ± 4	✓	✓	×	×	×	1	ROT
DC519281	5.576	100 ± 80	70 ± 10	60 ± 30	53 ± 9	×	✓	×	×	×	2	UNC
DC552206	5.502	138 ± 23	322 ± 8	52 ± 13	61 ± 17	✓	✓	×	✓	×	2	ROT
DC627939	4.533	170 ± 90	278 ± 4	50 ± 30	66 ± 8	✓	✓	×	×	×	2	UNC
DC683613	5.542	170 ± 40	353 ± 2	58 ± 30	49 ± 19	✓	×	×	✓	×	3	UNC
DC733857	4.545	87 ± 27	84 ± 16	84 ± 19	74 ± 1	×	✓	×	✓	×	3	UNC
DC773957	5.677	101 ± 11	35 ± 5	76 ± 11	66 ± 19	✓	✓	×	×	×	2	UNC
DC818760	4.561	94 ± 2	90 ± 5	74 ± 2	68 ± 9	✓	✓	✓	✓	✓	2	MER
DC848185	5.293	149 ± 11	320 ± 9	53 ± 9	52 ± 1	✓	×	×	✓	×	3	DIS
DC873321	5.154	118 ± 5	281 ± 9	73 ± 6	65 ± 10	✓	×	×	✓	×	2	MER
DC873756	4.546	121 ± 19	298 ± 1	42 ± 10	39 ± 27	✓	×	×	✓	×	2	DIS
DC881725	4.578	140 ± 40	324 ± 9	76 ± 33	48 ± 11	✓	✓	×	✓	×	1	ROT
VC5100537582	4.55	60 ± 90	77 ± 8	40 ± 50	49 ± 4	×	✓	×	✓	×	3	UNC
VC5100541407	4.563	69 ± 15	69 ± 7	59 ± 11	62 ± 10	×	×	×	✓	×	2	UNC
VC5100559223	4.563	167 ± 28	11 ± 5	75 ± 26	49 ± 4	✓	×	×	×	×	3	UNC
VC5100822662	4.521	0 ± 80	11 ± 15	40 ± 50	53 ± 7	×	✓	×	✓	×	2	MER
VC5100994794	4.58	55 ± 27	243 ± 9	69 ± 16	49 ± 17	✓	✓	×	✓	×	3	UNC
VC5101209780	4.57	23 ± 16	31 ± 13	57 ± 12	71 ± 8	✓	✓	×	✓	×	2	MER
VC5101218326	4.574	51 ± 25	9 ± 2	54 ± 27	44 ± 4	×	×	×	×	×	3	DIS
VC510786441	4.463	4 ± 6	1 ± 3	65 ± 7	67 ± 10	✓	✓	×	✓	×	2	UNC
VC5110377875	4.551	146 ± 18	147 ± 7	56 ± 15	50 ± 6	✓	✓	×	✓	×	1	ROT
VC5180966608	4.53	125 ± 34	311 ± 9	45 ± 22	52 ± 5	×	×	×	✓	×	2	UNC
VE530029038	4.43	130 ± 60	306 ± 7	50 ± 50	47 ± 15	✓	✓	×	✓	×	1	UNC
J0817	4.26	65 ± 24	93 ± 24	58 ± 23	48 ± 5	✓	✓	×	✓	×	—	ROT
HZ9	5.541	83 ± 22	17 ± 10	57 ± 14	59 ± 6	✓	✓	×	×	×	—	ROT

Результаты для ротаторов

Source	R [kpc]	v_{rot} [km s^{-1}]	σ_v [km s^{-1}]	M_{dyn} [$M_\odot$]
CG32	1.17	117.43 ± 20.71	39.06 ± 14.95	$(3.8 \pm 2.3) \times 10^9$
	3.5	115.04 ± 26.96	19.14 ± 12.47	$(1.1 \pm 0.5) \times 10^{10}$
DC396844	1.25	120.88 ± 10.74	44.42 ± 7.75	$(4.2 \pm 2.3) \times 10^9$
	3.75	80.42 ± 17.66	19.84 ± 11.75	$(5.6 \pm 2.6) \times 10^9$
DC494057	1.04	78.44 ± 10.25	53.24 ± 6.21	$(1.5 \pm 0.8) \times 10^9$
	3.13	80.31 ± 12.75	44.98 ± 7.1	$(4.7 \pm 1.7) \times 10^9$
DC552206	1.11	71.28 ± 21.74	116.65 ± 11.85	$(1.3 \pm 1.0) \times 10^9$
	3.32	164.98 ± 20.23	67.4 ± 13.24	$(2.1 \pm 0.6) \times 10^{10}$
	5.53	172.84 ± 27.63	65.34 ± 14.61	$(3.8 \pm 1.3) \times 10^{10}$
DC881725	1.15	98.37 ± 9.54	40.45 ± 6.94	$(2.6 \pm 1.4) \times 10^9$
	3.44	62.07 ± 12.54	48.4 ± 7.77	$(3.1 \pm 1.3) \times 10^9$
VC.7875	1.28	118.97 ± 8.1	47.04 ± 5.69	$(4.2 \pm 2.2) \times 10^9$
	3.84	102.85 ± 19.84	60.84 ± 12.74	$(9.4 \pm 4.0) \times 10^9$
J0817	0.95	247.46 ± 8.87	32.17 ± 11.36	$(1.4 \pm 0.7) \times 10^{10}$
	2.84	252.09 ± 14.94	35.98 ± 10.47	$(4.2 \pm 0.9) \times 10^{10}$
HZ9	0.54	155.85 ± 16.84	71.1 ± 8.38	$(3.0 \pm 1.7) \times 10^9$
	1.61	156.77 ± 19.02	75.12 ± 9.22	$(9.2 \pm 2.7) \times 10^9$
	2.68	176.63 ± 25.45	4.82 ± 8.0	$(1.9 \pm 0.6) \times 10^{10}$